



Published in final edited form as:

Cancer Discov. 2013 December ; 3(12): 1378–1393. doi:10.1158/2159-8290.CD-13-0005.

Hypoxia induces phenotypic plasticity and therapy resistance in melanoma via the tyrosine kinase receptors ROR1 and ROR2

Michael P. O'Connell¹, Katie Marchbank¹, Marie R. Webster¹, Alexander A. Valiga¹, Amanpreet Kaur¹, Adina Vultur¹, Ling Li¹, Meenhard Herlyn¹, Jessie Villanueva², Qin Liu², Xiangfan Yin², Sandy Widura¹, Janelle Nelson¹, Nivia Ruiz^{1,*}, Tura C. Camilli^{3,**}, Fred E. Indig³, Keith T. Flaherty⁴, Jennifer A. Wargo^{4,***}, Dennie T. Frederick⁴, Zachary A. Cooper^{4,***}, Suresh Nair⁵, Ravi K. Amaravadi⁶, Lynn M. Schuchter⁶, Giorgos C. Karakousis⁶, Wei Xu⁶, Xiaowei Xu⁶, and Ashani T. Weeraratna^{1,*},***

¹Tumor Metastasis and Microenvironment Program, The Wistar Institute, Philadelphia, PA

²Molecular and Cellular Oncogenesis Program, The Wistar Institute, Philadelphia, PA

³The National Institute on Aging, National Institutes of Health, Baltimore, MD

⁴Dana Farber/Harvard Cancer Center, Boston, MA

⁵Lehigh Valley Health Network, Allentown, PA

⁶Abramson Cancer Center, University of Pennsylvania, Philadelphia, PA

Abstract

An emerging concept in melanoma biology is that of dynamic, adaptive phenotype switching, where cells switch from a highly proliferative, poorly invasive phenotype to a highly invasive, less proliferative one. This switch may hold significant implications not just for metastasis, but also for therapy resistance. We demonstrate that phenotype switching and subsequent resistance can be guided by changes in expression of receptors involved in the non-canonical Wnt5A signaling pathway, ROR1 and ROR2. ROR1 and ROR2 are inversely expressed in melanomas and negatively regulate each other. Further, hypoxia initiates a shift of ROR1-positive melanomas to a more invasive, ROR2-positive phenotype. Notably, this receptor switch induces a 10-fold decrease in sensitivity to BRAF inhibitors. In melanoma patients treated with the BRAF inhibitor, Vemurafenib, Wnt5A expression correlates with clinical response and therapy resistance. These data highlight the fact that mechanisms that guide metastatic progression may be linked to those that mediate therapy resistance.

Introduction

The theory of dynamic, adaptive phenotype switching is based on the observation that unlike many other solid tumors, melanomas appear to down regulate signaling programs associated with proliferation in order to migrate (1, 2). These proliferative signaling programs are uniquely defined by genes involved in melanocyte differentiation and pigment production,

****To Whom Correspondence Should Be Addressed:* Ashani T. Weeraratna, Ph.D., Tumor Microenvironment and Metastasis Program, The Wistar Institute, 3601 Spruce Street, Philadelphia, PA 19104, Office: 215 495 6937, Fax: 215 495 6938, aweeraratna@wistar.org.

*Current Address: Hospital de la Concepcion, San Germain, PR 00683

**Current Address: FDA/CDER, 29 Lincoln Drive, Bethesda, MD 20892

***Current Address: Department of Surgical Oncology and Genomic Medicine, University of Texas M.D. Anderson Cancer Center, Houston, TX, 77030.

Conflict of Interest Statement: No known conflicts of interest exist.

such as MART1 and GP100, which are controlled by the transcription factor MITF. MITF has been shown to be critical for the transformation of melanocytes and the growth and proliferation of primary melanomas. However, the expression of MITF and its downstream effectors MART1 and GP100 are often decreased in metastatic melanomas (2, 3). The role of MITF in phenotype switching has been the subject of much investigation. MITF can repress invasion via the regulation of *Dial* and subsequently p27kip1. Targeted loss of MITF increases both tumorigenesis (4) and metastatic potential, via increases in EMT markers such as Snail, the reorganization of the actin cytoskeleton, and an increase in ROCK-dependent invasion (5). Hypoxia decreases the levels of MITF, as well as other melanocytic markers, driving the switch from a proliferative to an invasive phenotype (5, 6).

One of the other pathways intimately involved in the switch from a proliferative to an invasive phenotype in melanomas is the Wnt signaling pathway, which has also been shown to regulate the expression of MITF (7). Canonical Wnt signaling transduces signals that result in the stabilization of β -catenin, which is critical for the initial stages of melanoma development. In melanoma development, β -catenin stabilization is required to bypass melanocyte senescence (8), which results in melanocyte hyperproliferation, the activation of MITF and, ultimately, transformation and tumor growth (7). However, the role of β -catenin in metastasis remains controversial. Forced β -catenin stabilization, in the very distinct genetic context of concomitant BRAF and PTEN mutations (9), promotes melanoma metastasis. This is supported by an additional study that shows that in an N-Ras driven model of murine melanoma, stabilization of β -catenin promotes metastasis (10). However, the same study shows that β -catenin can inhibit the migration of melanoma cells and of melanocytes, via the induction of MITF, underscoring the complexity of the role of β -catenin in melanoma metastasis and invasion. In human melanoma cells, a recent study demonstrates that Wnt5A, when expressed in melanoma cells that have Frizzled 7, can activate β -catenin, also leading to an increase in invasion (11). Conversely, immunohistochemical analysis has demonstrated that nuclear β -catenin is a positive prognostic marker for melanomas (12). Further data also suggest that melanomas with active canonical Wnt signaling are less metastatic (and more proliferative) than those with active non-canonical Wnt signaling (12, 13), and at least two recent studies demonstrate that silencing β -catenin increases invasion and *in vivo* metastasis (14, 15). Recently, it has also been shown that BRAF mutant melanomas that express elevated β -catenin are more sensitive to BRAF inhibitors (16). This suggests that not only may β -catenin expression predict a better prognosis in melanomas, but also a better response to targeted therapy. Overall, we speculate that the cohort of receptors, co-receptors and Wnt ligands guide the fate of melanoma cells, and may predict their response to therapy (17).

The role of the non-canonical Wnt signaling molecule, Wnt5A, is more predictable than β -catenin, at least in melanomas. Multiple studies have shown that Wnt5A is increased in metastatic melanomas, and can drive the invasion of melanoma cells (3, 11, 18–20). Overexpression of Wnt5A results in decreased proliferation and increased metastases in a B16 melanoma mouse model, as well as in human melanoma cells (3, 19, 21, 22). In addition to affecting metastasis, overexpression of Wnt5A downregulates the transcription of melanocytic antigens (MART1, GP100 and their promoters PAX3 and MITF) via the activation of STAT3 (3), resulting in a decrease in pigment, proliferation and antigenicity of melanoma cells. All of these signaling changes downstream of Wnt5A promote the phenotype switch from early tumorigenesis to an advanced metastatic state. Further, these effects require the expression of the tyrosine kinase receptor ROR2, and in the absence of ROR2, Wnt5A is unable to promote melanoma metastasis (21).

ROR2 is a tyrosine kinase receptor that specifically transduces Wnt5A signaling (23). Only one other member of this family has been identified thus far, ROR1 (24). ROR1 and ROR2

have an amino acid homology of 58%, and are single pass transmembrane proteins with immunoglobulin-like, cysteine-rich and kringle domains on the extracellular portion (24). The intracellular domain contains both tyrosine and serine-threonine kinase domains (25). ROR1 has been shown to be an important molecule in the pathogenesis of cancers such as acute lymphoblastic leukemia (26) and lung cancer (27), where it drives the survival and proliferation of these two cancer types. Like Wnt5A, ROR1 appears to play the opposite role in melanomas than it does in breast cancers. Wnt5A acts in a tumor suppressive manner in breast cancers, but promotes the invasion and metastasis of melanoma cells. We show in this study that ROR1 inhibits the invasion of melanoma cells, but in breast cancer, ROR1 has been shown to promote an EMT and subsequent metastasis (28). Further, ROR1 is associated with the increased growth of breast cancer cells (29). This discrepancy between breast cancers and melanomas has always been striking, but remains unexplained, and points again to the importance of cellular context in Wnt signaling.

Since ROR2 is critical for Wnt5A-mediated metastasis in melanomas (21), we sought to determine what role ROR1 might play in melanoma progression. Here we show that despite its strong homology to ROR2, ROR1 is associated with the proliferative phenotype during early tumorigenesis of melanomas, rather than the invasive phenotype of metastatic disease, and therefore has alternative roles to ROR2 in melanoma progression. This is supported by recent data showing that ROR1 may play a role in the survival of melanoma cells (30). Intriguingly, we found that hypoxia guides the switch between the expression of the two highly homologous receptors, ROR1 and ROR2, providing a functional demonstration that hypoxia may act as one of the “triggers” for phenotype switching in melanoma crisis. We also demonstrate that this phenotypic switch may hold significant implications not only for tumor invasion, but also for therapy resistance.

Results

ROR1 marks a poorly invasive phenotype in melanoma cells

Wnt5A and ROR2 levels are elevated in melanomas and are indicative of increased metastatic potential (21, 22). Phenotype switching in melanomas was first defined by Hoek *et al.*, who analyzed the gene expression profiles of several short-term cultures of melanoma cells (2). They found that their databases could be divided into cell lines that had low (Cohort A) *versus* high (Cohort C) invasive potential. Cells in Cohort A (poorly invasive) were much more proliferative than those in Cohort C. Markers of proliferation, such as MITF, were expressed in Cohort A (proliferative) and Wnt5A was expressed in Cohort C (invasive), and these markers clearly defined the proliferative from the invasive phenotype. We used this data set largely because the invasive and proliferative phenotypes have been confirmed experimentally (2). We analyzed whether ROR1 gene expression was significantly decreased in this gene expression set, and found that ROR1 was more highly expressed in the proliferative cohort compared to the invasive cohort (Figure 1A). In these samples, as opposed to Wnt5A expression (Supplementary Figure S1A), the melanocytic markers MITF (Supplementary Figure S1B), GP100 (Supplementary Figure S1C), DCT (Supplementary Figure S1D) and MART1 (Supplementary Figure S1E) were also decreased in the more invasive cohort, suggesting that ROR1 is inversely associated with the invasive phenotype. We selected ten melanoma cell lines that were either poorly invasive or highly invasive, and compared mRNA expression levels of ROR1 (Figure 1B) and ROR2 (Figure 1C) using Q-RT-PCR. Our results confirmed the microarray data, demonstrating an increase in ROR1 in poorly invasive samples, as compared to ROR2, which is elevated in highly invasive melanoma cells. We next compared ROR1 protein levels in 6 melanoma cell lines, in which we have previously established invasive capacity (3, 21, 22). ROR1 was not expressed in the three melanoma cell lines that are highly invasive (WM793, 1205LU and

M93-047), but the 3 that are poorly invasive (UACC1273, WM35 and WM1799) have robust ROR1 expression (Figure 1D). We further confirmed this using a 3-D skin reconstruct model, where artificial skin is built using keratinocytes, fibroblasts and either melanocytes or melanoma cells of differing stages of progression (31). Serial sections were stained for ROR1, Wnt5A and ROR2. ROR1 was expressed in melanocytes and in poorly invasive WM35 cells (Figure 1E, melanocytes and WM35). ROR2 and Wnt5A, however, were expressed in more invasive WM793 cells (Figure 1E, WM793) and in highly invasive 1205LU melanoma cells (Figure 1E, 1205LU). These data are consistent with the gene expression data (Figure 1A,B,C) that indicate that ROR1 is expressed in proliferative, poorly invasive cells, and its expression is decreased in metastatic cells.

Wnt5A regulates ROR1 expression

Since ROR1 is downregulated in metastatic melanomas and Wnt5A increases both ROR2 expression and melanoma metastasis, we asked whether Wnt5A could directly regulate levels of ROR1. Treatment with recombinant Wnt5A (rWnt5A) resulted in a significant down-regulation of ROR1 mRNA in two poorly invasive cell lines (UACC1273 and G361) as measured by Q-RT-PCR (Figure 2A). To confirm this at the protein level, we performed both Western blot analysis and surface biotinylation assays. Surface biotinylation assays determine the amount of ROR1 expression that is present at the cell surface, and is available for ligand binding. ROR1 was decreased by rWnt5A treatment of Wnt5A-low UACC1273 cells, in contrast to ROR2, which was increased by rWnt5A treatment of these cells (21). In the high Wnt5A, high ROR2, metastatic cell lines UACC903, M93-047 and UACC647, we found no ROR1 expression (Figure 2B). To determine how quickly ROR1 was degraded upon Wnt5A treatment, we treated Wnt5A low G361 and UACC1273 cells with rWnt5A over a time course. ROR1 protein levels decreased significantly as quickly as 5 minutes in both lines (Figure 2C, Supplementary Figure S2A). This suggested that the protein was being rapidly degraded upon Wnt5A treatment, and its decrease was not simply a result of decreased transcription.

To determine by which route ROR1 was degraded upon rWnt5A treatment, we analyzed the lysosomal and proteasomal degradation pathways. Immunofluorescent studies demonstrated that there is a level of ROR1 associated with lysosomes, even in the absence of rWnt5A (Supplementary Figure S2A). However, the colocalization of ROR1 with lysosomes did not increase with rWnt5A treatment (Supplementary Figure S2A). We next used the inhibitors Lys05 (32) and Bafilomycin 1 to inhibit lysosome function. Inhibition of lysosomal function with either of those inhibitors did not increase the accumulation of ROR1, suggesting that lysosomal degradation is not the primary mechanism for Wnt5A-mediated ROR1 degradation (Supplementary Figure S2B). In order to determine if ROR1 was being degraded via proteasomes, we treated ROR1-positive melanoma cells with the proteasome inhibitor MG132. In the presence of MG132, ROR1 accumulated in the cells (Figure 2D, E, MG132). Treatment with rWnt5A decreased ROR1 expression (Figure 2D, E, +rWnt5A), but in the presence of MG132 could no longer do so (Figure 2D, E, MG132 + rWnt5A).

Many of the downstream events of Wnt5A are mediated via the activation of PKC, and the PKC isoforms activated by Wnt5A are PKC α , β II and γ . (22). To determine whether PKC activation plays a role in the Wnt5A-mediated down-regulation of ROR1, we manipulated the activity of PKC in cells using the PKC inhibitor GO6983 (targeted to the conventional PKC isoforms). First, we treated Wnt5A high UACC903 cells with GO6983. In control conditions, there was very little expression of ROR1, and Wnt5A was localized to endosomes, from where we have previously shown it is signaling (21). When PKC was inhibited (GO6983), Wnt5A was released from the endosomes and the levels of ROR1 were increased (Supplementary Figure S3A). Western blot analysis shows that inhibition of PKC, even in Wnt5A low cells, can also increase the levels of ROR1, suggesting that even the low

levels of Wnt5A in these cells can regulate ROR1 (Figure 2F). Next, we treated Wnt5A low cells (G361, UACC1273) with rWnt5A in the presence or absence of PKC inhibitors, and asked how that affected ROR1 levels. In the absence of GO6983, cells have high levels of ROR1 (Figure 2G, Supplementary Figure S3B, UT). Treatment with rWnt5A decreased ROR1 expression (Figure 2G, Supplementary Figure S3B, +rWnt5A). In the presence of only the GO6983 inhibitor, ROR1 expression was unaffected (Figure 2G, Supplementary Figure S3B, +GO, 1 μ M). However, upon pre-treatment of the cells with GO6983, rWnt5A was less efficient at decreasing ROR1, suggesting that PKC is required for the Wnt5A-mediated degradation of ROR1 (Figure 2G, Supplementary Figure S3B, GO + rWnt5A). Taken together, these data suggest that Wnt5A targets ROR1 to proteasomes for degradation in a PKC-dependent manner.

Loss of ROR1 drives melanoma cell invasion

Since ROR1 expression is decreased in metastatic melanoma cells, we sought to determine whether ROR1 knockdown could increase invasion. We used two different ROR1 siRNAs targeted to two different regions of the gene (ROR1_5, ROR1_6). ROR1 knockdown resulted in an increase in both Wnt5A and ROR2 expression in multiple cell lines (Figure 3A). To determine whether knockdown of ROR2 could similarly affect ROR1 expression, we knocked down ROR2 using a previously validated siRNA. ROR2 knockdown increased ROR1 expression (Figure 3B, Supplementary Figure S4A). To determine the effects of ROR1 knockdown on invasion, we subjected cells to 3D spheroid invasion assays, where cells were embedded in collagen. Knockdown of ROR1 significantly increased the invasion of poorly invasive WM35, WM983B and WM1799 melanoma cells (Figure 3C). Simultaneous knockdown of both ROR1 and ROR2 ablated invasion, suggesting that the primary way in which ROR1 mediates invasion is via the increase of ROR2 (Figure 3C). These data suggest that ROR1 and ROR2 are reciprocally regulated and play opposing roles in melanoma invasion.

To translate these results *in vivo* we knocked down ROR1 in WM35 and WM983B cells, and injected those cells subcutaneously in nude mice. WM35 cells were allowed to grow for 60 days. For the first 20 days the knockdown of ROR1 significantly (**p<0.001) reduced the growth rate of these tumors. After that time, the growth rate increased to the level of the control, presumably due to the siRNA no longer being effective (Figure 3D). WM983B cells, which grow faster than WM35 cells, were allowed to grow for 33 days. In these cells, ROR1 knockdown less significantly affected the growth rate of these tumors, but the trend was the same (Supplementary Figure S4B). Animals bearing WM35 xenografted cells were euthanized and examined for metastases. Knockdown of ROR1 spurred the formation of visceral metastases by WM35 cells (Figure 3E,F) cells. In this cell line, knocking down ROR1 spurred the formation of metastases in the majority of animals (9 out of 10). Interestingly, in animals xenografted with the control WM35 cells, previously thought to be radial growth phase and not metastatic, we found evidence of one animal with a small number of metastases in the lungs.

Hypoxia induces the switch from ROR1 to ROR2, increasing invasion

Our data suggest that melanoma cells switch from a ROR1-positive to an ROR2-positive phenotype during melanoma invasion, we wanted to understand what initiated this switch. As melanoma cells invade deeper into the skin, they encounter an increasingly hypoxic microenvironment and the protein HIF1 α has been shown to be elevated as melanomas progress (33). HIF1 α plays a role in ROR2 upregulation (34) and is also inversely correlated with MITF expression in melanomas (5, 6, 35), so we analyzed the role of hypoxia in the induction of ROR1 to ROR2 phenotype switching. First, we confirmed that exposure of melanoma cells to hypoxia (2% O₂) increases their invasion using motility (scratch-wound)

assays (Figure 4A). HIF1 α expression was increased in the cells by 6 hours as expected (Figure 4B). This upregulation is concomitant with a decrease in MITF and an increase in Wnt5A, suggesting that the phenotype switch occurs upon exposure to hypoxic conditions (Figure 4C). To determine whether HIF1 α is responsible for Wnt5A upregulation following hypoxia, we knocked down HIF1 α using siRNA (Figure 4D). This resulted in the inability of hypoxia to induce Wnt5A expression (Figure 4E) suggesting that HIF1 α is required for Wnt5A expression. These experiments were performed with 2 different siRNAs at 20nM (Supplementary Figure S5A).

We next queried whether the ROR receptors are also affected by hypoxia. In the presence of hypoxia, ROR1 was downregulated (Figure 4F,G), where ROR2 was upregulated (Figure 4H). In the absence of HIF1 α , ROR2 was decreased (Figure 4I). The hypoxia-mediated upregulation of ROR2 was blocked by Wnt5A silencing in highly invasive cell lines (Figure 4J). In poorly invasive cell lines, there was little effect of Wnt5A silencing on ROR2 or HIF1 α during normoxic conditions, presumably because Wnt5A levels are already so low (Supplementary Figure S5B). These data suggest that hypoxia is one factor that can drive the switch from a non-invasive ROR1-positive phenotype to an invasive, ROR2-positive phenotype. Further, these data indicate that the upregulation of ROR2 via HIF1 α requires Wnt5A.

Wnt5A upregulates Siah2, stabilizing HIF1 α levels, resulting in increases in ROR2

In order to understand how HIF1 α might work in cohort with Wnt5A to increase the expression of ROR2 during hypoxia, we looked for downstream signaling mediators in common between Wnt5A and HIF1 α . A common signaling intermediate in hypoxia and Wnt5A signaling is the E3 ubiquitin ligase, Siah2. Wnt5A regulation of canonical Wnt signaling occurs predominantly via upregulation of Siah2, resulting in a GSK3- β -independent degradation of β -catenin (36). Siah2 plays an important role during hypoxia, as it inhibits prolyl hydroxylases, resulting in the stabilization of HIF1 α (37). Additionally, Siah2 is upregulated in metastatic melanomas (38), so we hypothesized that Siah2 upregulation may be downstream of Wnt5A in melanomas, just as it is during development.

We examined Siah2 expression in our melanoma cell lines. Siah2 expression was increased in Wnt5A high UACC903 and M93-047 cells, as compared to Wnt5A low UACC1273 cells (Figure 5A) and knockdown of Wnt5A decreased Siah2 expression (Figure 5B). This suggests that Wnt5A can indeed regulate Siah2 expression. To determine whether Siah2 is activated by hypoxia in melanoma cells, we exposed cells to hypoxia for 6 and 24 hours. Siah2 was increased in both poorly invasive (UACC1273) and highly invasive (M93-047) melanoma cells (Figure 5C). To determine whether Wnt5A upregulation of Siah2 plays a role during hypoxia-initiated phenotype switching, we knocked down Wnt5A in invasive melanoma cells. When exposed to hypoxia, these cells were no longer able to upregulate Siah2 (Figure 5D) and HIF1 α expression (Figure 5E) was also decreased. This implies that Wnt5A is required for the activation of Siah2 during hypoxia, and acts in a positive feedback loop with HIF1 α .

Since β -catenin is a target of Siah2, we sought to determine whether Wnt5A requires Siah2 to affect β -catenin levels in melanoma cells. We have previously shown that Wnt5A overexpression in proliferative phenotype melanoma cells can cause a decrease or dysregulation of β -catenin expression in those cells (39). Further, β -catenin mRNA expression is downregulated in highly invasive compared to poorly invasive melanoma cell lines (2), and β -catenin expression can predict better patient outcome (13). rWnt5A treatment of Wnt5A low UACC1273 cells resulted in a decrease of β -catenin expression, which, like ROR1, was dependent on proteasomal function (Figure 5F). rWnt5A treatment of G361 cells also decreased β -catenin expression (Supplementary Figure S5C). We then

knocked down Siah2 in poorly invasive melanoma cells (Supplementary Figure S5D), and showed that in the presence of Siah2 siRNA, β -catenin levels begin to accumulate (Figure 5G, Supplementary Figure S5E). In the absence of Siah2, Wnt5A can no longer affect β -catenin expression or localization (Figure 5G, Supplementary Figure S5E).

Taken together, these data demonstrate that hypoxia can drive the switch from ROR1 to ROR2 positivity in melanoma cells, and that Wnt5A, via Siah2, plays a critical role in the hypoxic induction of phenotype switching. These data provide evidence that microenvironmental regulation of non-canonical Wnt signaling is essential for the phenotypic plasticity of melanoma cells, and further, these data identify HIF1 α as a novel target of non-canonical Wnt signaling. Our data also suggest that Siah2 may perform its function as a promoter of the metastatic phenotype of melanoma cells both via its stabilization of HIF1 α and its down-regulation of β -catenin (see schematic in Figure 5H).

Phenotype switching in BRAF mutant cells decreases sensitivity to BRAF inhibitors

We then asked what the clinical implications of the observed phenotype switch might be. Previous studies have demonstrated that activated β -catenin expression sensitizes BRAF mutant melanoma cells to Vemurafenib therapy (16). We hypothesized that, conversely, Wnt5A high melanoma cells with BRAF mutations might prove to be less sensitive to Vemurafenib therapy. To analyze this, we identified cell lines with BRAFV600E mutations and measured their Wnt5A and ROR2 status, as well as their sensitivity to BRAF inhibitors. Out of 11 BRAF mutant cell lines tested, with low and high Wnt5A, there was a significant correlation between BRAF inhibitor resistance and Wnt5A expression ($p=0.017$) (Figure 6A). Treating PLX-sensitive 451LU melanoma cells with rWnt5A prior to the administration of PLX4720 increased the resistance of these cells to PLX4720 by almost 2-fold (Figure 6B). ROR2 is the tyrosine kinase receptor responsible for Wnt5A signal transduction in melanomas, and the expression of this receptor was also increased in PLX-resistant cells (Figure 6C).

To determine whether knockdown of ROR2 would sensitize Wnt5A high cells to the BRAF inhibitor, PLX4720, we treated resistant or partially resistant Wnt5A-high, ROR2-high cells (1205Lu, UACC62, FS4) with siRNA directed against ROR2 (Supplementary Figure S6A), and analyzed the cells for response to therapy. Knockdown of ROR2 sensitized melanoma cells for therapy *in vitro* (Figure 6D, Supplementary Figure S6B,C). To determine whether these results could be translated *in vivo*, we took partially resistant 1205LU melanoma cells and treated them with either control or ROR2 siRNA. These cells were then injected into nude mice subcutaneously. SiRNA was delivered to the tumor site once a week by injection, a method we have previously shown to be effective in maintaining ROR2 gene silencing (21). ROR2 downregulation was maintained in these tumors as well (Supplementary Figure S6D). Mice were divided into 4 groups: 1) control siRNA + PLX4720-laced chow (AIN-76A, with 417 mg/kg PLX4720), 2) control siRNA + untreated chow (AIN-76A), 3) ROR2siRNA + PLX4720-laced chow (AIN-76A, with 417 mg/kg PLX4720) and 4) ROR2 siRNA + untreated chow (AIN-76A). Pre-treatment of PLX-resistant 1205Lu cells with ROR2 siRNA dramatically increased the response to PLX4720 *in vivo* compared to control siRNA (Figure 6E). In contrast, knockdown of ROR2 did not significantly affect the proliferation of tumor cells in the absence of PLX4720 (Figure 6E).

Next, we asked whether ROR1 was decreased in resistant cells and whether the knockdown of ROR1 could affect the response to PLX4720. ROR1 expression was decreased in PLX4720-resistant cells (Figure 6F). We performed a similar experiment using WM35 and WM983B melanoma cells, which both express ROR1 and are sensitive to PLX. Animals bearing xenografted tumors, either control siRNA or ROR1 siRNA treated, were fed chow containing PLX4720, after tumor development. Tumors were measured for a period of 3

weeks. The results show that the knockdown of ROR1 significantly ($*p<0.01$) decreased sensitivity to PLX4720 both in WM35 cells (Figure 6G) and in WM983B cells (Supplementary Figure S6E, $p<0.004$). These data imply that inhibition of ROR2 in conjunction with BRAF inhibitors may target a subset of patients not previously responsive to these drugs. Also, the loss of ROR1 increases the resistance to PLX4720, further confirming the observation that the microenvironment can guide a phenotype switch to a more aggressive tumor type.

Wnt5A expression correlates with resistance in human tumor samples

To further confirm and extend these findings, we sought to assess whether the expression of Wnt5A could predict patient response to Vemurafenib in a small cohort of patients ($n=24$). Robust clinical response to Vemurafenib is defined as 30% response or higher. To account for human error in measuring response, we extended this definition of clinical response to include samples of 35% or higher. We were able to identify 9 patients with 33% response or lower to Vemurafenib, and 15 patients with a 38% or higher response to the drug. Examples of Wnt5A staining in correlation to therapeutic response are shown in Figure 7A. Treatment, time to progression, and survival were assessed in this cohort of patients and the data are summarized in Supplementary Table 1. Even in this small cohort of patients, the results were significant: 7 out of 9 patients who demonstrated less than 33% clinical response to Vemurafenib had positive expression of Wnt5A, from 1–3+ intensity. Only 2 of the remaining 15 patients (38% response or greater) exhibited any Wnt5A expression (1–2+ intensity) as shown in Figure 7B, giving a statistical significance of $p=0.002$. It should be noted that while ROR1 and ROR2 status would also likely provide further evidence of resistance to therapy, the antibodies available are not robust enough for reliable FFPE analysis.

If Wnt5A truly confers clinical resistance to BRAF inhibitors, then we would predict that Wnt5A-positive cells might be selected for in patients who relapse (become resistant) while on therapy. To test this we acquired 12 patient samples that had undergone BRAF inhibitor therapy, and for whom we had pre-therapy and post-therapy, relapsed lesions. We scored the levels of Wnt5A expression in these samples, and found that 8/12 post-relapse samples had increased Wnt5A positivity compared to pre-therapy lesions (i.e., positivity in a larger percentage of the tumor). Two examples are shown in Figure 7C. In these 8 patients, positivity increased from an average of 6% of the tumor cells being positive for Wnt5A pre-therapy, to an average of 52% of the tumor cells being positive post-relapse ($p=0.016$). In the remaining four patients, one sample increased from 25–30% positivity (which we did not consider significant and therefore scored this unchanged), one remained the same (5% positivity, pre- and post-), one decreased from 16% positivity to 10% positivity, and one decreased from 5% positivity to no positivity. All the data are summarized in Supplementary Table 2. When considering all 12 tumors together, the overall increase in Wnt5A staining went from 8% positivity pre-therapy to 38% positivity post-relapse, and was significant at $p=0.018$. Interestingly, in one sample for which we had pre-treatment, on-treatment and post-relapse samples, Wnt5A staining increased from 0 to 80% positivity in the on-treatment sample, to 100% positivity (and an increase from 1–2+ intensity) in the post-relapse sample.

We also examined resistant cells in vitro. We took resistant subclones of the PLX-sensitive cell line WM983B (40), which are initially sensitive to BRAF inhibitors. This acquired resistance can be demonstrated by the failure of PLX4720 to inhibit ERK activation in the resistant cells compared to the parental cells (Figure 7D). Next, we analyzed the resistant subclones for their ROR1, ROR2 and Wnt5A status. Compared to the parental cell lines, resistant subclones lost ROR1 expression and increased their levels of Wnt5A and ROR2 (Figure 7E). We asked whether treatment of sensitive cells with Wnt5A could increase ERK activation, and indeed, 451LU and WM983B cells treated with Wnt5A have increased PO_4 -

ERK expression (Figure 7F), suggesting that activation of Wnt5A may provide an alternate route to maintain MAPK signaling in the face of BRAF inhibition. These data suggest that the Wnt5A pathway plays a role in resistance to BRAF inhibitors, and may represent both a viable target for adjuvant therapy in melanoma patients harboring the BRAF mutation, as well as a valuable prognostic indicator of therapy response. These data highlight the fact that the mechanisms that underlie the phenotypic plasticity leading to increased invasion and those that underlie therapy resistance are very tightly connected.

Discussion

Understanding the mechanisms that underlie phenotype switching and the role it plays in the generation of aggressive, therapy-resistant melanoma cells is of increasing importance in melanoma biology. We have long postulated that melanoma cells make decisions whether to “grow or go”. While this has obvious implications for metastasis, we are just beginning to appreciate the extent to which metastatic signaling programs may also guide therapy resistance. Changes in molecules such as MITF and Wnt5A guide a switch to a mesenchymal, invasive population of melanoma cells. In this study we show that the mechanisms by which Wnt5A guides one outcome (metastasis) may have a significant impact on another (therapy resistance).

The Wnt signaling pathway consists of several Wnts that signal via β -catenin (canonical Wnt signaling) and others that signal via PKC, Ca^{2+} and Jnk (non-canonical Wnt signaling). The dynamic between the different members of this family of proteins is of increasing interest in melanoma biology. Wnt5A, a non-canonical Wnt, does not appear to play a role in melanocyte transformation, yet is critical for driving melanoma metastasis. The role of β -catenin in melanocyte transformation and melanoma growth is abundantly clear- its role in metastasis is less so, with most studies indicating that β -catenin signaling decreases during progression (7, 8, 41, 42). Further, the suppression of β -catenin has been shown to increase invasion in melanoma cells (43). In contrast, a recent study indicates that stabilizing β -catenin in the context of both a BRAF mutation, and a PTEN deletion increases metastatic progression (9), but it is unclear how often this defined genetic profile (BRAF^{V600E}/PTEN^{-/-}/CTNNB1^{STA}) occurs in melanoma patients. Overall, most data imply that during melanoma invasion, melanoma cells switch from a canonical Wnt signaling pathway to a non-canonical Wnt signaling one.

While Wnt ligands can be quite promiscuous, the co-receptor, ROR2, is faithful in activating the non-canonical Wnt signaling pathway. Here, we describe for the first time the regulation and loss of a tyrosine kinase receptor not previously associated with melanoma, the ROR1 receptor. In other cancers, ROR1 plays a pro-tumorigenic role, driving the growth, survival and tumorigenic transformation of met-driven cancers including gastric, renal and non-small cell lung cancers (27, 44–47). Taken together, these data point to a role for ROR1 in driving tumor growth. However, the role of ROR1 in melanomas has not been previously assessed. We show that knockdown of ROR1 decreases melanoma cell proliferation *in vivo*, implicating it in growth. We show that Wnt5A can signal to increase the proteasomal degradation of ROR1, such that ROR1 is decreased during invasion. When ROR1 expression is decreased, that of Wnt5A and ROR2 increases, and this corresponds to increases in invasion and metastasis. These data indicate that while ROR1 may play a role in melanoma cell growth, its loss is necessary for invasion, underscoring the increasingly common observation that factors driving tumor growth may be quite distinct from those that drive tumor metastasis.

Hypoxia has been shown to be a driving force for the metastatic progression of melanomas (38, 48). Additionally, ROR2 is postulated to be a target of HIF1 α (34). We hypothesized

that as tumors become larger, and increase their hypoxic regions, the activation of ROR2 could drive increased aggression, increased Wnt5A signaling and decreases in ROR1. Indeed, our data show that in the presence of hypoxia, ROR1 expression decreases, and expression of ROR2 and Wnt5A increases, in a HIF1 α -dependent manner. Surprisingly, we found that Wnt5A plays a critical role in the stabilization of HIF1 α via the E3 ubiquitin ligase Siah2. Siah2 is activated during hypoxia via phosphorylation of its serine/threonine residues, and acts to stabilize HIF1 α . Research has shown that Wnt5A can act via ROR2 to increase Siah2 phosphorylation and activity (49) and we confirm that finding in this study. However, we also show for the first time that through this activation of Siah2, Wnt5A is also able to stabilize HIF1 α , highlighting HIF1 α as a novel downstream target of Wnt5A.

In addition to increasing invasion, hypoxic upregulation of Wnt5A/ROR2 has another important corollary. By upregulating Siah2, Wnt5A is able to downregulate β -catenin. β -catenin expression has been shown to sensitize melanoma cells to BRAF inhibitors (16), leading us to postulate that if Wnt5A signaling decreased β -catenin, then Wnt5A should make melanoma cells more resistant to BRAF inhibitor therapy. Indeed, our data indicate that Wnt5A plays a role in intrinsic resistance as melanoma patients tend to respond poorly to Vemurafenib if they express higher levels of Wnt5A. Although this is a small sample size, Wnt5A expression in pre-treatment biopsies accurately predicted response to BRAF inhibitors in 7/9 non-responder (less than 35% response) patient samples, and in 13/15 responders. Furthermore, analysis of patient tumors pre- and post- BRAF inhibitor therapy demonstrate significant increases in Wnt5A expression. This may be attributable to the fact that Wnt5A-positive cells are more intrinsically resistant to BRAF inhibitors, therefore, it is this resistant subpopulation that continues to survive during BRAF inhibitor therapy, and ultimately dominates. Alternatively, inhibition of BRAF in Wnt5A high cells may drive increased MAPK signaling via the Wnt5A pathway.

The link between the mechanisms that underlie tumor metastasis and therapy resistance is not well defined, however it is clear that tumors that are more aggressive are likely to be more resistant to therapy. Yet, predicting which tumor is likely to metastasize faster when comparing stage IV tumors is challenging. Thus, the use of Wnt5A as a prognostic marker for both time of progression free survival as well as therapy response may be of great clinical utility. Other data from our laboratory further implicate Wnt5A in resistance to other forms of therapy, and this is mediated by Wnt5A control of β -catenin (Webster et al, in submission). This is supported by a recent study that implicates β -catenin in resistance not only to BRAF inhibitors, but also to MEK inhibitors (50). It should be noted that increases in Wnt5A expression observed post-therapy were observed in melanoma patients who received both BRAF inhibitors and ERK inhibitors as well (Supplementary Table 2). Thus, targeting the Wnt5A/ROR2 pathway may not only increase initial sensitivity to BRAF inhibition as demonstrated in our animal studies, but may also provide a useful mechanism for targeting relapsing tumors. Ongoing work in our laboratory seeks to identify small molecule inhibitors of ROR2, hoping that we can use them to generate more effective and durable responses to Vemurafenib. Importantly, as the ROR2 pathway also drives melanoma metastasis, such inhibitors could be of great clinical benefit in the 50% of patients that do not carry the BRAFV600E mutation.

EXPERIMENTAL PROCEDURES

(Extended Experimental Procedures are available as Supplementary Information)

Cell Culture—UACC1273EV, UACC903, M93-047 and UACC647 cells were maintained in RPMI (Invitrogen, Carlsbad, CA). G-361 cells were maintained in McCoy's 5A media (Invitrogen). All the above cell line media were supplemented with 10% FBS, 100 units/ml penicillin and streptomycin and 4 mM L-glutamine. 451LU and WM983B cells were

maintained in DMEM with 5% FBS. 451LU BR (BRAF inhibitor resistant) and WM983B BR cells were maintained in DMEM with 5% FBS containing 1 μ M/ml PLX4720. Melanocytes were maintained in Medium 254CF containing Human Melanocyte Growth Supplement-2 without PMA (HMGS-2) (Invitrogen). WM35, WM793, 451LU and 1205LU cells were maintained in MCDB153 (Sigma, St Louis, MO)/L-15 (Cellgro, Manassas, VA) (4:1 ratio) supplemented with 2% FBS and 1.6 mM CaCl_2 . Fibroblasts were maintained in DMEM, supplemented with 10% FBS. Keratinocytes were maintained in keratinocyte SFM supplemented with human recombinant Epidermal Growth Factor 1–53 (EGF 1–53) and Bovine Pituitary Extract (BPE) (Invitrogen). Cell lines were cultured at 37°C in 5% CO_2 and the medium was replaced as required. Cell stocks were fingerprinted using AmpFLSTR® Identifiler® PCR Amplification Kit from Life Technologies™ at The Wistar Institute Genomics Facility. Although it is desirable to compare the profile to the tissue or patient of origin, our cell lines were established over the course of 40 years, long before acquisition of normal control DNA was routinely performed. However, each STR profile is compared to our internal database of over 200 melanoma cell lines as well as control lines such as HeLa and 293T. STR profiles are available upon request. Cell culture supernatants were mycoplasma tested using a Lonza MycoAlert assay at the University of Pennsylvania Cell Center Services. For rWnt5A treatment, concentrations and treatment times were as previously established to be optimal for these cells (Dissanayake et al., 2007). For inhibition of lysosomes and 26s proteasomes and hypoxic treatment doses and times see Extended Experimental Procedures.

siRNA Transfection—HP-validated CTRL, Wnt5A, HIF1 α (2), Siah2 (2), ROR1 (2) and ROR2 siRNAs (20 – 200 nmoles, Qiagen, Valencia, CA) were transfected into cells using Lipofectamine (Invitrogen) as previously described (O'Connell et al., 2009). siRNA sequences are listed in Supplementary Table 1.

Organotypic 3D Skin Reconstructs—Organotypic 3D skin reconstructs were generated as previously described (Li et al, 2011). Melanocytes and melanoma cell lines at different stages of progression (RGP, VGP, and metastatic) were used to generate the reconstructs. Please refer to the Extended Experimental Procedures for details.

Cellular Proliferation and Motility Assays—MTS assays were used to determine cell proliferation. Motility assays were performed as previously described (O'Connell et al, 2010). Please refer to the Extended Experimental Procedures for details.

3D Spheroid Assays—The formation of spheroids is outlined in the Extended Experimental Procedures section. Collagen plugs were fixed in 1:10 formalin for 10 minutes, processed into paraffin blocks, and sectioned onto slides.

Immunofluorescence (IF)—Primary antibodies used were: Wnt5A (10 μ g/ml) (R&D Systems, Minneapolis, MN), ROR1 (2.5 μ g/ml), ROR2 (2.5 μ g/ml), HIF1 α (0.5 μ g/ml), phospho- β -catenin (T41/S45) (1 μ g/ml), β -catenin (0.5 μ g/ml) (Cell Signaling, Danvers, MA), MART1 (2 μ g/ml) (Thermo Scientific, Fremont, CA) and LAMP2 (5 μ g/ml) (Abcam, Cambridge, MA). For details please refer to the Extended Experimental Procedures.

Immunohistochemistry (IHC)—Patient samples were collected under IRB exemption approval for protocol #EX21205258-1. Samples were stained for Wnt5A expression using a biotinylated Wnt5A antibody (R&D Systems). For details please refer to the Extended Experimental Procedures.

Mouse ROR2 siRNA PLX4720 assay—All animal experiments were approved by the Institutional Animal Care and Use Committee (IACUC) (IACUC #112503X_0) and were performed in an Association for the Assessment and Accreditation of Laboratory Animal Care (AAALAC) accredited facility. 1205LU cells were transfected with CTRL or ROR2 siRNA as described above. 48 hours following transfection, 7.5×10^5 cells suspended in PBS/Matrigel (500 $\mu\text{g}/\text{ml}$) were subcutaneously injected into each 6 week old female athymic nude mouse (Charles River Laboratories, Wilmington, MA). Mice were injected intratumorally with 150 nM siRNA once a week until euthanized. When resulting tumors reached 200 mm^3 , mice were fed either AIN-76A chow or AIN-76A chow containing 417 mg/kg PLX4720. Tumor sizes were measured every 3–4 days using digital calipers, and tumor volumes were calculated using the following formula: $\text{volume} = 0.5 \times (\text{length} \times \text{width}^2)$. Time-to-event (survival) was determined by a 5-fold increase in baseline volume ($\sim 1000 \text{mm}^3$) and was limited by the development of skin necrosis. Upon the occurrence of necrosis, mice were euthanized. Tumors were harvested, paraffin embedded and sectioned.

Mouse ROR1 siRNA PLX4720 assay—WM35 and WM983B cells were transfected with CTRL or ROR1 siRNA (2 different siRNAs) as described above. 48 hours following transfection, 1×10^6 cells suspended in PBS/Matrigel (500 $\mu\text{g}/\text{ml}$) were subcutaneously injected into each 6 week old female athymic nude mouse (Charles River Laboratories). Mice were injected intratumorally with 100 nM siRNA once a week until euthanized. After 33 days of growth, mice injected with WM35 cells were fed either AIN-76A chow or AIN-76A chow containing 417 mg/kg PLX4720. Mice injected with WM983B cells were fed AIN-76A chow containing 417 mg/kg PLX4720. Tumor sizes were measured every 3–5 days using digital calipers, and tumor volumes were calculated using the following formula: $\text{volume} = 0.5 \times (\text{length} \times \text{width}^2)$. Time-to-event (survival) was determined by a 5-fold increase in baseline volume ($\sim 1000 \text{mm}^3$) and was limited by the development of skin necrosis. Upon the occurrence of necrosis, mice were euthanized. For all mice, tumors were harvested and for WM35 mice the lungs were also analyzed for metastasis.

Statistical Analysis—For in vitro studies, Student's t test or ANOVA was performed using at least three independent experiments. For in vivo studies, the fold change in tumor volume after treatment at 14 days relative to baseline was used to evaluate the treatment effect. Means, standard deviations (SD) and medians were calculated and distributions of data were examined to ascertain whether normal theory methods are appropriate. The Kruskal-Wallis test and post-hoc Wilcoxon rank-sum test were used for multiple comparisons among experimental groups. Bonferroni's adjusted p-values were calculated and used to determine the statistical significance. For patient samples, paired T-tests were used to calculate significance. Stata 12.0 (StatCorp LP, College Station, TX, USA) was used for data analysis. Significance was designated as follows: *, $p < 0.05$; **, $p < 0.01$; ***, $p < 0.001$.

Supplementary Material

Refer to Web version on PubMed Central for supplementary material.

Acknowledgments

We thank Dr. Gideon Bollag for access to the PLX4720 laced AIN-76A chow. We thank Dr. Dario Altieri for critical reading of the manuscript and helpful comments. We thank the Histology and the Imaging Core Facilities of the Wistar Institute. This work was supported in part by funds from the National Institute on Aging Intramural Research Program and the PA Department of Health (CURE) funding and the Joanna M Nicolay Foundation (AK).

Financial Support: This work was supported in part by funds from the National Institute on Aging Intramural Research Program (FEI, TCC, JN) and the PA Department of Health (CURE) funding (ATW, MPO, KM, AV, NR,

QL, XF, SW) and the Joanna M Nicolay Foundation (AK). Additional support for other authors comes from PHS 2 T32 CA 9171-36 (MRW), 1K23CA120862 (RKA), and CA25874 (MH).

Abbreviations

ANOVA	analysis of variance
EMT	epithelial to mesenchymal transition
FFPE	formaldehyde-fixed, paraffin- embedded
mRNA	messenger ribonucleic acid
PCR	Polymerase Chain Reaction
PO₄	phosphorylated
Q-RT-PCR	Quantitative Real Time Polymerase Chain Reaction
RGP	radial growth phase
siRNA	small interfering RNAs
STDEV	standard deviation
VGP	vertical growth phase

Reference List

1. Ghislin S, Deshayes F, Middendorp S, Boggetto N, Alcaide-Loridan C. PHF19 and Akt control the switch between proliferative and invasive states in melanoma. *Cell Cycle*. 2012; 11:1634–1645. [PubMed: 22487681]
2. Hoek KS, Schlegel NC, Brafford P, Sucker A, Ugurel S, Kumar R, et al. Metastatic potential of melanomas defined by specific gene expression profiles with no BRAF signature. *Pigment Cell Res*. 2006; 19:290–302. [PubMed: 16827748]
3. Dissanayake SK, Olkhanud PB, O'Connell MP, Carter A, French AD, Camilli TC, et al. Wnt5A regulates expression of tumor-associated antigens in melanoma via changes in signal transducers and activators of transcription 3 phosphorylation. *Cancer Res*. 2008; 68:10205–10214. [PubMed: 19074888]
4. Cheli Y, Giuliano S, Botton T, Rocchi S, Hofman V, Hofman P, et al. Mitf is the key molecular switch between mouse or human melanoma initiating cells and their differentiated progeny. *Oncogene*. 2011; 30:2307–2318. [PubMed: 21278797]
5. Cheli Y, Giuliano S, Fenouille N, Allegra M, Hofman V, Hofman P, et al. Hypoxia and MITF control metastatic behaviour in mouse and human melanoma cells. *Oncogene*. 2012; 31:2461–2470. [PubMed: 21996743]
6. Widmer DS, Hoek KS, Cheng PF, Eichhoff OM, Biedermann T, Raaijmakers MI, et al. Hypoxia Contributes to Melanoma Heterogeneity by Triggering HIF1alpha-Dependent Phenotype Switching. *J Invest Dermatol*. 2013
7. Goodall J, Martinozzi S, Dexter TJ, Champeval D, Carreira S, Larue L, et al. Brn-2 expression controls melanoma proliferation and is directly regulated by beta-catenin. *Mol Cell Biol*. 2004; 24:2915–2922. [PubMed: 15024079]
8. Delmas V, Beermann F, Martinozzi S, Carreira S, Ackermann J, Kumasaka M, et al. Beta-catenin induces immortalization of melanocytes by suppressing p16INK4a expression and cooperates with N-Ras in melanoma development. *Genes Dev*. 2007; 21:2923–2935. [PubMed: 18006687]
9. Damsky WE, Curley DP, Santhanakrishnan M, Rosenbaum LE, Platt JT, Gould Rothberg BE, et al. beta-catenin signaling controls metastasis in Braf-activated Pten-deficient melanomas. *Cancer Cell*. 2011; 20:741–754. [PubMed: 22172720]
10. Gallagher SJ, Rambow F, Kumasaka M, Champeval D, Bellacosa A, Delmas V, et al. Beta-catenin inhibits melanocyte migration but induces melanoma metastasis. *Oncogene*. 2013; 32:2230–2238. [PubMed: 22665063]

11. Grossmann AH, Yoo JH, Clancy J, Sorensen LK, Sedgwick A, Tong Z, Ostanin K, Rogers A, Grossmann KF, Tripp SR, Thomas KR, D'Souza-Schorey C, Odelberg SJ, Li DY. The small GTPase ARF6 stimulates b-catenin transcriptional activity during WNT5A-mediated melanoma invasion and metastasis. *Science Signaling*. 2013;6.
12. Bachmann IM, Straume O, Puntervoll HE, Kalvenes MB, Akslen LA. Importance of P-cadherin, beta-catenin, and Wnt5a/frizzled for progression of melanocytic tumors and prognosis in cutaneous melanoma. *Clin Cancer Res*. 2005; 11:8606–8614. [PubMed: 16361544]
13. Chien AJ, Moore EC, Lonsdorf AS, Kulikauskas RM, Rothberg BG, Berger AJ, et al. Activated Wnt/beta-catenin signaling in melanoma is associated with decreased proliferation in patient tumors and a murine melanoma model. *Proc Natl Acad Sci U S A*. 2009; 106:1193–1198. [PubMed: 19144919]
14. Arozarena I, Bischof H, Gilby D, Belloni B, Dummer R, Wellbrock C. In melanoma, beta-catenin is a suppressor of invasion. *Oncogene*. 2011; 30:4531–4543. [PubMed: 21577209]
15. Lee DJ, Kang DH, Choi M, Choi YJ, Lee JY, Park JH, et al. Peroxiredoxin-2 represses melanoma metastasis by increasing E-cadherin/beta-catenin complexes in adherens junctions. *Cancer Res*. 2013
16. Biechele TL, Kulikauskas RM, Toroni RA, Lucero OM, Swift RD, James RG, et al. Wnt/beta-catenin signaling and AXIN1 regulate apoptosis triggered by inhibition of the mutant kinase BRAFV600E in human melanoma. *Sci Signal*. 2012; 5 ra3.
17. Webster MR, Weeraratna AT. A Wnt-er migration: the confusing role of beta-catenin in melanoma metastasis. *Sci Signal*. 2013; 6:pe11. [PubMed: 23532332]
18. Da Forno PD, Pringle JH, Hutchinson P, Osborn J, Huang Q, Potter L, et al. WNT5A expression increases during melanoma progression and correlates with outcome. *Clin Cancer Res*. 2008; 14:5825–5832. [PubMed: 18794093]
19. Dissanayake SK, Wade M, Johnson CE, O'Connell MP, Leotlela PD, French AD, et al. The Wnt5A/protein kinase C pathway mediates motility in melanoma cells via the inhibition of metastasis suppressors and initiation of an epithelial to mesenchymal transition. *J Biol Chem*. 2007; 282:17259–17271. [PubMed: 17426020]
20. Jenei V, Sherwood V, Howlin J, Linnskog R, Sahlholm A, Axelsson L, et al. A t-butyloxycarbonyl-modified Wnt5a-derived hexapeptide functions as a potent antagonist of Wnt5a-dependent melanoma cell invasion. *Proc Natl Acad Sci U S A*. 2009; 106:19473–19478. [PubMed: 19901340]
21. O'Connell MP, Fiori JL, Xu M, Carter AD, Frank BP, Camilli TC, et al. The Orphan Tyrosine Kinase Receptor, ROR2, Mediates Wnt5A Signaling in Metastatic Melanoma. *Oncogene*. 2009
22. Weeraratna AT, Jiang Y, Hostetter G, Rosenblatt K, Duray P, Bittner M, et al. Wnt5a signaling directly affects cell motility and invasion of metastatic melanoma. *Cancer Cell*. 2002; 1:279–288. [PubMed: 12086864]
23. Oishi I, Suzuki H, Onishi N, Takada R, Kani S, Ohkawara B, et al. The receptor tyrosine kinase Ror2 is involved in non-canonical Wnt5a/JNK signalling pathway. *Genes Cells*. 2003; 8:645–654. [PubMed: 12839624]
24. Katoh M. Comparative genomics on ROR1 and ROR2 orthologs. *Oncol Rep*. 2005; 14:1381–1384. [PubMed: 16211313]
25. Masiakowski P, Carroll RD. A novel family of cell surface receptors with tyrosine kinase-like domain. *J Biol Chem*. 1992; 267:26181–26190. [PubMed: 1334494]
26. Bicocca VT, Chang BH, Kharabi Masouleh B, Muschen M, Loriaux MM, Druker BJ, et al. Crosstalk between ROR1 and the Pre-B Cell Receptor Promotes Survival of t(1;19) Acute Lymphoblastic Leukemia. *Cancer Cell*. 2012; 22:656–667. [PubMed: 23153538]
27. Yamaguchi T, Yanagisawa K, Sugiyama R, Hosono Y, Shimada Y, Arima C, et al. NKX2-1/TTF1/TTF-1-Induced ROR1 is required to sustain EGFR survival signaling in lung adenocarcinoma. *Cancer Cell*. 2012; 21:348–361. [PubMed: 22439932]
28. Cui B, Zhang S, Chen L, Yu J, Widhopf GF 2nd, Fecteau JF, et al. Targeting ROR1 Inhibits Epithelial-Mesenchymal Transition and Metastasis. *Cancer Res*. 2013; 73:3649–3660. [PubMed: 23771907]

29. Zhang S, Chen L, Cui B, Chuang HY, Yu J, Wang-Rodriguez J, et al. ROR1 is expressed in human breast cancer and associated with enhanced tumor-cell growth. *PLoS One*. 2012; 7:e31127. [PubMed: 22403610]
30. Hojjat-Farsangi M, Ghaemimanesh F, Daneshmanesh AH, Bayat AA, Mahmoudian J, Jeddi-Tehrani M, et al. Inhibition of the receptor tyrosine kinase ROR1 by anti-ROR1 monoclonal antibodies and siRNA induced apoptosis of melanoma cells. *PLoS One*. 2013; 8:e61167. [PubMed: 23593420]
31. Berking C, Herlyn M. Human skin reconstruct models: a new application for studies of melanocyte and melanoma biology. *Histol Histopathol*. 2001; 16:669–674. [PubMed: 11332722]
32. Amaravadi RK, Winkler JD. Lys05: a new lysosomal autophagy inhibitor. *Autophagy*. 2012; 8:1383–1384. [PubMed: 22878685]
33. Kuphal S, Winklmeier A, Warnecke C, Bosserhoff AK. Constitutive HIF-1 activity in malignant melanoma. *Eur J Cancer*. 2010; 46:1159–1169. [PubMed: 20185296]
34. Wright TM, Rathmell WK. Identification of Ror2 as a hypoxia-inducible factor target in von Hippel-Lindau-associated renal cell carcinoma. *J Biol Chem*. 2010; 285:12916–12924. [PubMed: 20185829]
35. Feige E, Yokoyama S, Levy C, Khaled M, Igras V, Lin RJ, et al. Hypoxia-induced transcriptional repression of the melanoma-associated oncogene MITF. *Proc Natl Acad Sci U S A*. 2011; 108:E924–E933. [PubMed: 21949374]
36. Topol L, Jiang X, Choi H, Garrett-Beal L, Carolan PJ, Yang Y. Wnt-5a inhibits the canonical Wnt pathway by promoting GSK-3-independent beta-catenin degradation. *J Cell Biol*. 2003; 162:899–908. [PubMed: 12952940]
37. Nakayama K, Qi J, Ronai Z. The ubiquitin ligase Siah2 and the hypoxia response. *Mol Cancer Res*. 2009; 7:443–451. [PubMed: 19372575]
38. Qi J, Nakayama K, Gaitonde S, Goydos JS, Krajewski S, Eroshkin A, et al. The ubiquitin ligase Siah2 regulates tumorigenesis and metastasis by HIF-dependent and -independent pathways. *Proc Natl Acad Sci U S A*. 2008; 105:16713–16718. [PubMed: 18946040]
39. Eichhoff OM, Weeraratna A, Zipser MC, Denat L, Widmer DS, Xu M, et al. Differential LEF1 and TCF4 expression is involved in melanoma cell phenotype switching. *Pigment Cell Melanoma Res*. 2011; 24:631–642. [PubMed: 21599871]
40. Villanueva J, Vultur A, Lee JT, Somasundaram R, Fukunaga-Kalabis M, Cipolla AK, et al. Acquired resistance to BRAF inhibitors mediated by a RAF kinase switch in melanoma can be overcome by cotargeting MEK and IGF-1R/PI3K. *Cancer Cell*. 2010; 18:683–695. [PubMed: 21156289]
41. Rimm DL, Caca K, Hu G, Harrison FB, Fearon ER. Frequent nuclear/cytoplasmic localization of beta-catenin without exon 3 mutations in malignant melanoma. *Am J Pathol*. 1999; 154:325–329. [PubMed: 10027390]
42. Takeda K, Yasumoto K, Takada R, Takada S, Watanabe K, Udono T, et al. Induction of melanocyte-specific microphthalmia-associated transcription factor by Wnt-3a. *J Biol Chem*. 2000; 275:14013–14016. [PubMed: 10747853]
43. Arozarena I, Sanchez-Laorden B, Packer L, Hidalgo-Carcedo C, Hayward R, Viros A, et al. Oncogenic BRAF induces melanoma cell invasion by downregulating the cGMP-specific phosphodiesterase PDE5A. *Cancer Cell*. 2011; 19:45–57. [PubMed: 21215707]
44. Baskar S, Kwong KY, Hofer T, Levy JM, Kennedy MG, Lee E, et al. Unique cell surface expression of receptor tyrosine kinase ROR1 in human B-cell chronic lymphocytic leukemia. *Clin Cancer Res*. 2008; 14:396–404. [PubMed: 18223214]
45. Gentile A, Lazzari L, Benvenuti S, Trusolino L, Comoglio PM. Ror1 is a pseudokinase that is crucial for Met-driven tumorigenesis. *Cancer Res*. 2011; 71:3132–3141. [PubMed: 21487037]
46. Rabbani H, Ostadkarampour M, Danesh Manesh AH, Basiri A, Jeddi-Tehrani M, Forouzes F. Expression of ROR1 in patients with renal cancer--a potential diagnostic marker. *Iran Biomed J*. 2010; 14:77–82. [PubMed: 21079657]
47. Zhang S, Chen L, Wang-Rodriguez J, Zhang L, Cui B, Frankel W, et al. The Onco-Embryonic Antigen ROR1 Is Expressed by a Variety of Human Cancers. *Am J Pathol*. 2012

48. Victor N, Ivy A, Jiang BH, Agani FH. Involvement of HIF-1 in invasion of Mum2B uveal melanoma cells. *Clin Exp Metastasis*. 2006; 23:87–96. [PubMed: 16826425]
49. MacLeod RJ, Hayes M, Pacheco I. Wnt5a secretion stimulated by the extracellular calcium-sensing receptor inhibits defective Wnt signaling in colon cancer cells. *Am J Physiol Gastrointest Liver Physiol*. 2007; 293:G403–G411. [PubMed: 17463182]
50. Conrad WH, Swift RD, Biechele TL, Kulikauskas RM, Moon RT, Chien AJ. Regulating the response to targeted MEK inhibition in melanoma: enhancing apoptosis in NRAS- and BRAF-mutant melanoma cells with Wnt/beta-catenin activation. *Cell Cycle*. 2012; 11:3724–3730. [PubMed: 22895053]

Significance

These data show for the first time that a single signaling pathway, the Wnt signaling pathway, can effectively guide the phenotypic plasticity of tumor cells, when primed to do so by a hypoxic microenvironment. Importantly, this increased Wnt5A signaling can give rise to a subpopulation of highly invasive cells that are intrinsically less sensitive to novel therapies for melanoma, and targeting the Wnt5A/ROR2 axis could improve the efficacy and duration of response for melanoma patients on Vemurafenib.

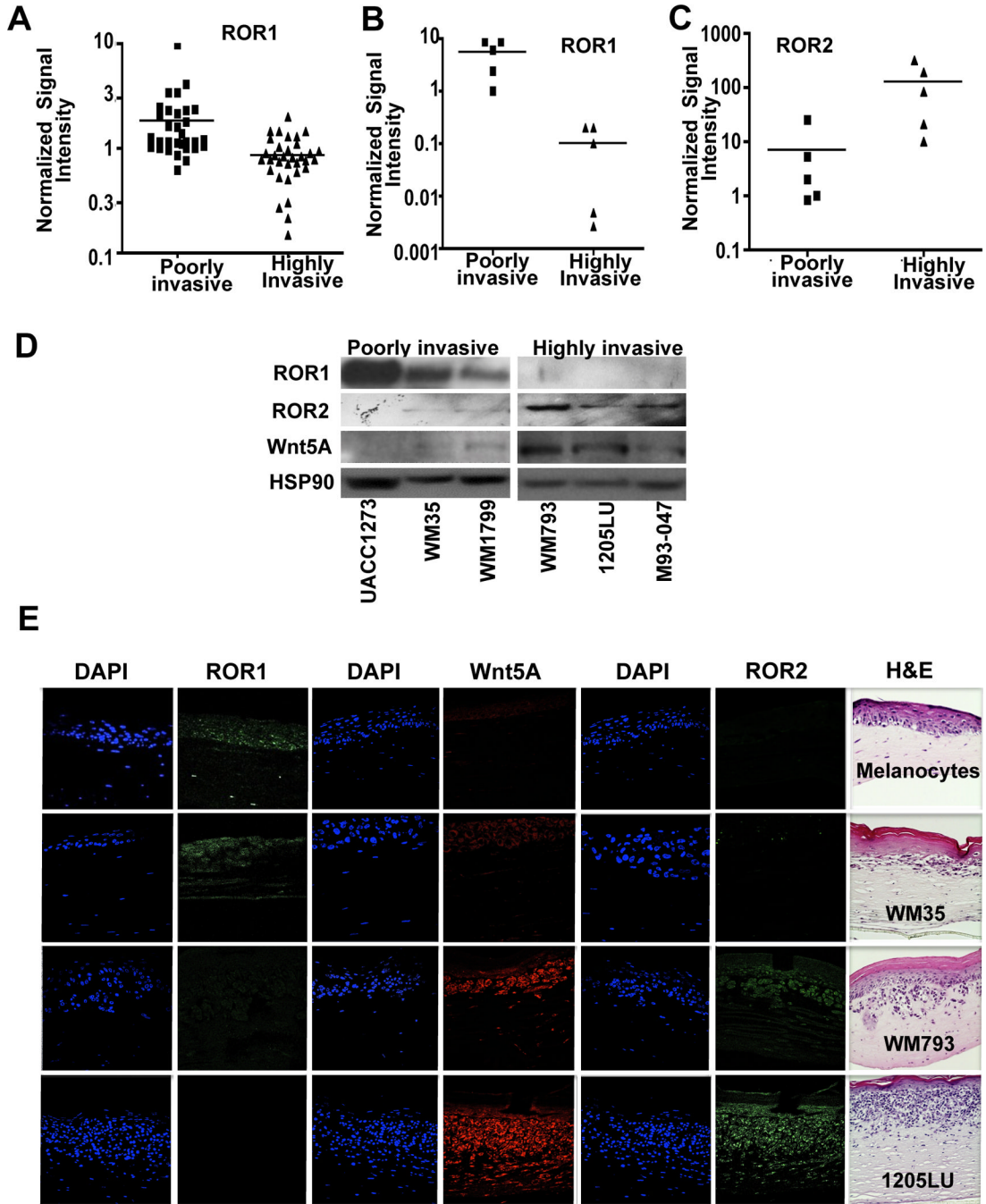


Figure 1. ROR1 Expression is Inversely Correlated to Wnt5A/ROR2

(A) Gene expression of ROR1 in multiple microarray databases of melanoma cell lines divided into a more proliferative, less metastatic cohort (Cohort A) *versus* a highly metastatic cohort (Cohort C). (***p*<0.001) (B) Quantitative real time PCR of ROR1 mRNA levels in a panel of poorly invasive compared to highly invasive cell lines (***p*<0.01, ****p*<0.001). (C) Quantitative real time PCR of ROR2 mRNA levels in a panel of poorly invasive compared to highly invasive cell lines (***p*<0.01, ****p*<0.001). (D) Western blot analysis of ROR1 and ROR2 expression in poorly invasive and highly invasive cell lines; densitometry is shown on the right. (E) Immunofluorescent analysis of ROR1 (green),

Wnt5A (red) and ROR2 (green) protein expression in organotypic 3D reconstruct models of melanocytes and melanoma cells in radial growth phase (RGP-WM35), vertical growth phase (VGP-WM793) and metastatic (MET-1205Lu) stages. Hematoxylin and Eosin (H&E) staining of organotypic 3D reconstruct models of melanocytes and melanoma cells in RGP, VGP and MET stages is shown on the right.

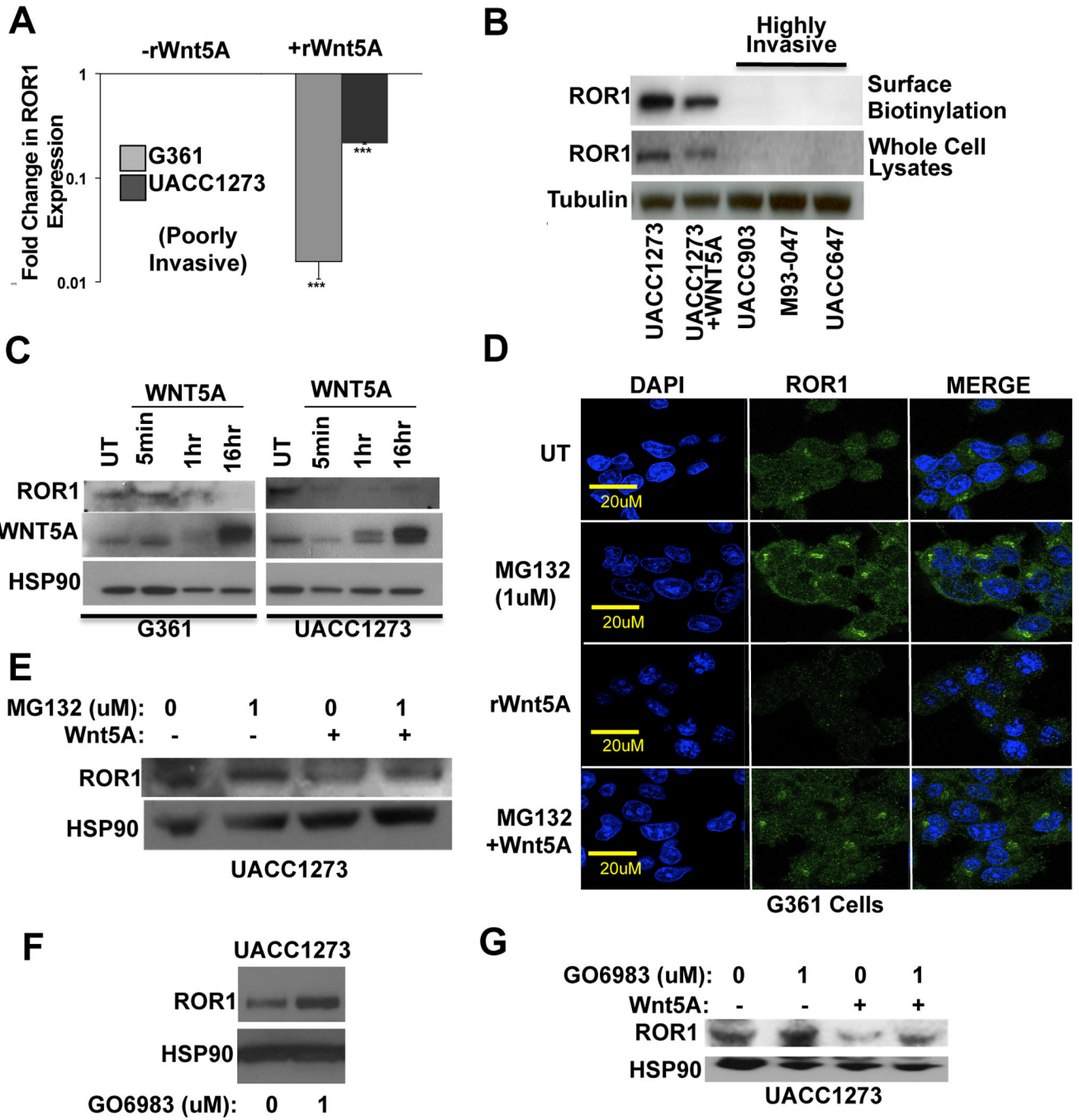


Figure 2. Wnt5A Decreases ROR1 Expression Through Proteasomal Degradation
 (A) Real-time PCR analysis of ROR1 mRNA levels in Wnt5A low UACC1273 and G361 cell lines +/- treatment with rWnt5A (200 ng/ml, 16 hours) (***)p<0.001; error bars=STDEV). (B) Surface biotinylation and Western blot analyses of ROR1 protein expression in UACC1273 cells (+/- rWnt5A) as well as metastatic UACC903, M93-047 and UACC647 cell lines. (C) Time course analysis (5 minutes, 1 hour, 16 hours) of ROR1, Wnt5A and HSP90 in G361 and UACC1273 cells. (D) Expression of ROR1 (green) protein in G361 cells following pre-treatment with the proteasome inhibitor (MG132, 10 μM, 1 hour) in the presence or absence of rWnt5A (200 ng/ml, 10 minutes). (E) Western blot analysis of ROR1 protein in UACC1273 cells following pre-treatment with the proteasome

inhibitor (MG132, 10 μ M, 1 hour) in the presence or absence of rWnt5A (200 ng/ml, 16 hours). (F) Western blot analysis of ROR1 in poorly invasive UACC1273 cells following treatment with the PKC inhibitor GO6983 (1 μ M, 17 hours). (G) Western blot analysis of ROR1 protein in UACC1273 cells following pre-treatment with the PKC inhibitor GO6983 (1 μ M, 17 hours) in the presence or absence of rWnt5A (200 ng/ml, 16 hours).

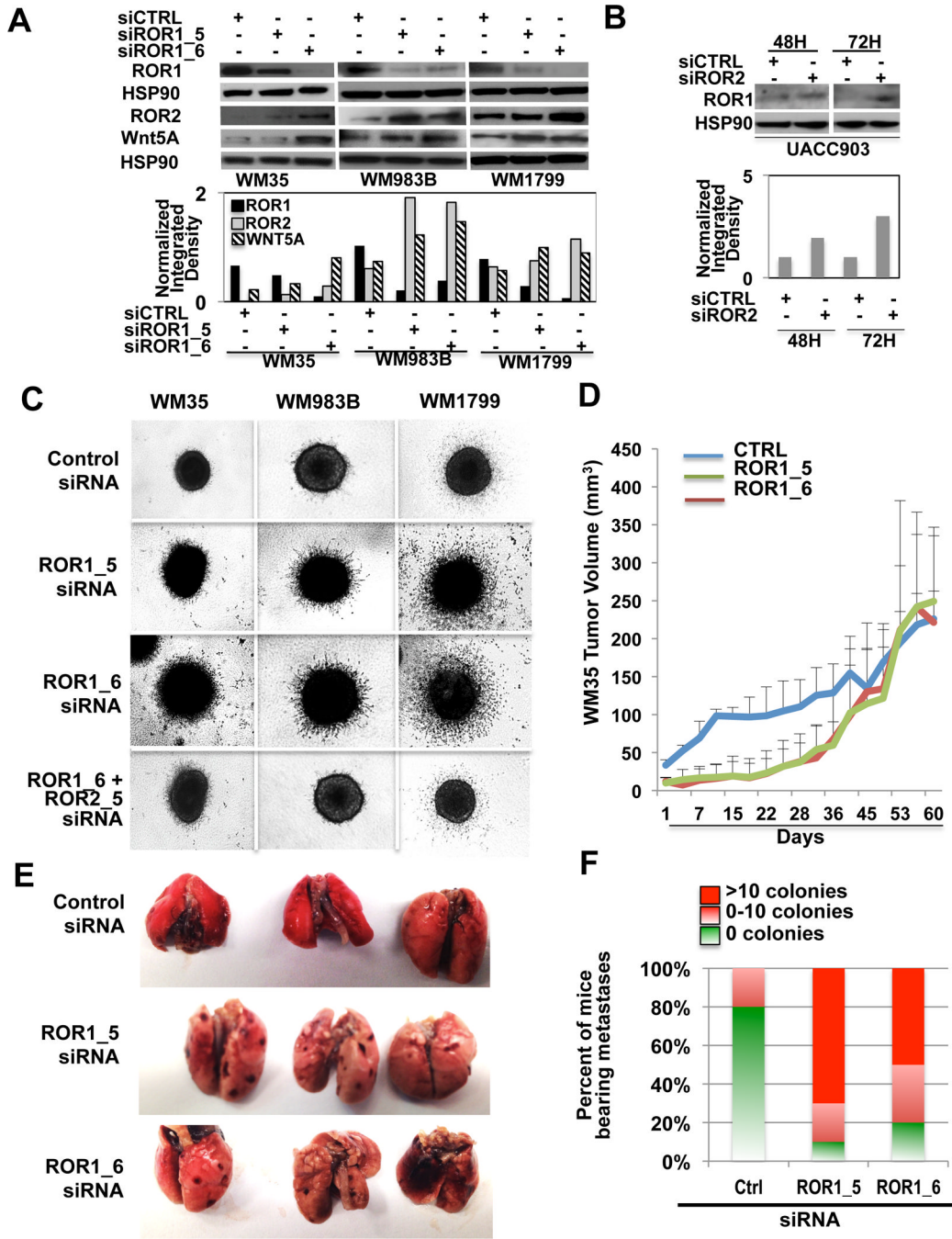


Figure 3. Knockdown of ROR1 Increases the Invasive Potential of Melanoma Cells *in vitro* and *in vivo*

(A) ROR1 protein expression examined by Western blot analysis following treatment with CTRL or ROR1 siRNA (using multiple siRNAs) for 72 hours in WM35, WM983B and WM1799 cells. (B) Expression of ROR1 following ROR2 knockdown after 48 and 72 hours in cells. (C) Invasive potential of WM35, WM983B and WM1799 cells following treatment with ROR1 siRNA assessed by 3D spheroid assays. (D) Tumor growth assay (*in vivo*) in WM35 cells following treatment with CTRL or ROR1 siRNA (2 different ROR1 siRNAs). (E) Representative images of lung metastases following treatment with CTRL or ROR1

siRNA. (F) Graphical representation of counts of metastatic colonies seen in lungs of CTRL, ROR1_5 or ROR1_6 siRNA treated mice.

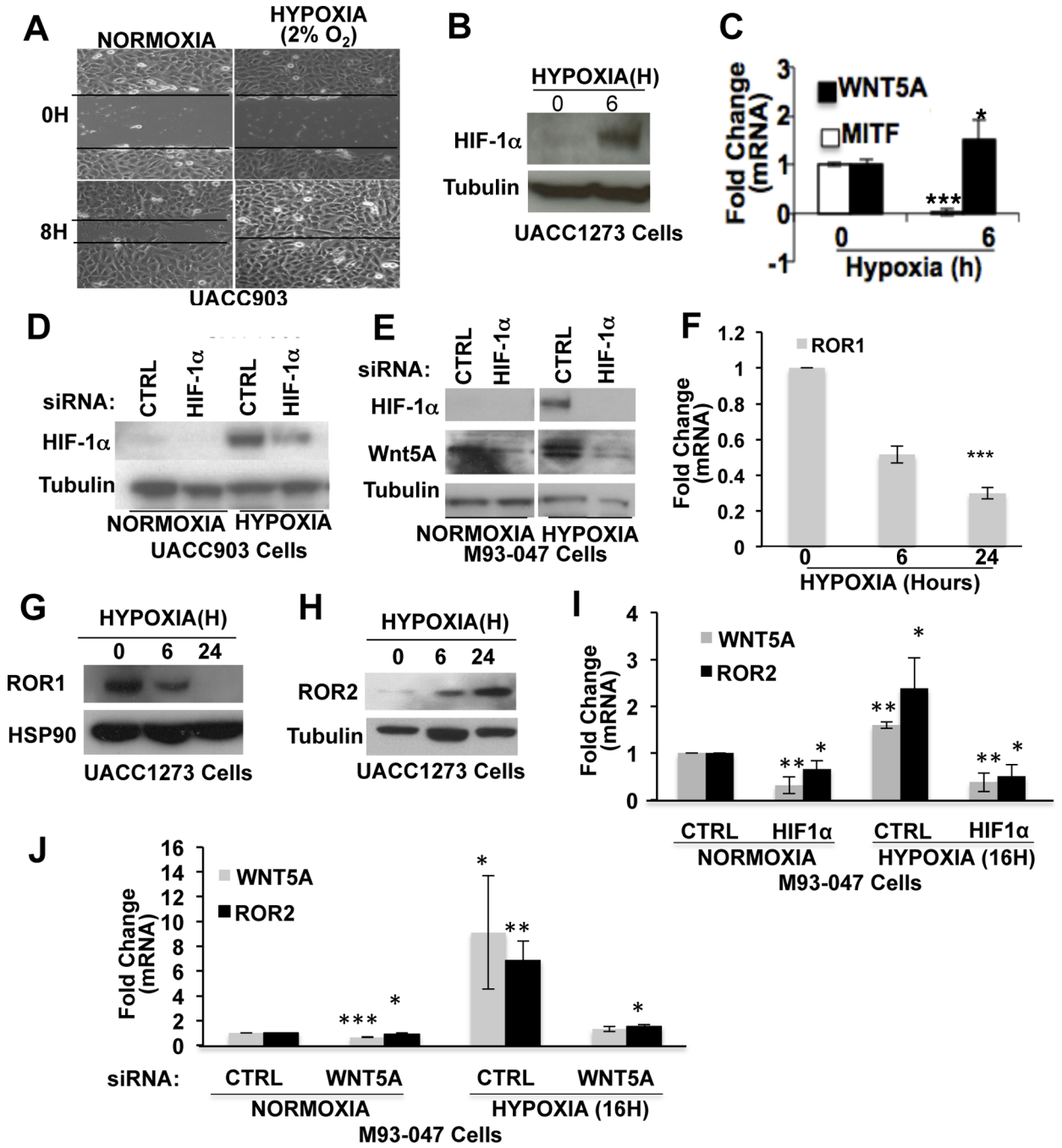


Figure 4. Hypoxia Induces a Switch in ROR Receptor Expression and Increases Wnt5A Expression and Motility

A) Wound healing assay of UACC903 cells seeded onto collagen coated plates and exposed to hypoxia (2% O₂). Cells were scratched and imaged at 0 and 8 hours. (B) Protein expression of HIF1α in UACC1273 cells following exposure to hypoxia (2% O₂) for 6 hours. (C) mRNA levels of Wnt5A and MITF following exposure to hypoxia (2% O₂, 6 hours) analyzed by real-time PCR (*p<0.05, ***p<0.001; error bars=STDEV). (D) Western blot analysis of HIF1α protein expression in UACC903 cells following treatment with CTRL or HIF1α siRNA under normoxic and hypoxic conditions. (E) Western blot analysis of HIF1α and Wnt5A protein expression in M93-047 cells following treatment with CTRL

or HIF1 α siRNA under normoxic and hypoxic conditions. (F) Real-time PCR analysis of ROR1 mRNA levels in UACC1273 cells following exposure to hypoxia (2% O₂, 6 hours and 48 hours) (**p<0.001; error bars=STDEV). Western blot analysis of ROR1 (G) and ROR2 (H) protein expression in UACC1273 cells following exposure to hypoxia. (I) Analysis of ROR2 and Wnt5A mRNA levels, by real-time PCR, following treatment with CTRL or HIF1 α siRNA in M93-047 cells (*p<0.05; error bars=STDEV). (J) Wnt5A and ROR2 mRNA levels assessed by real time PCR following treatment with CTRL or Wnt5A siRNA in M93-047 cells under normoxic or hypoxic conditions (*p<0.05, **p<0.01, ***p<0.001; error bars=STDEV).

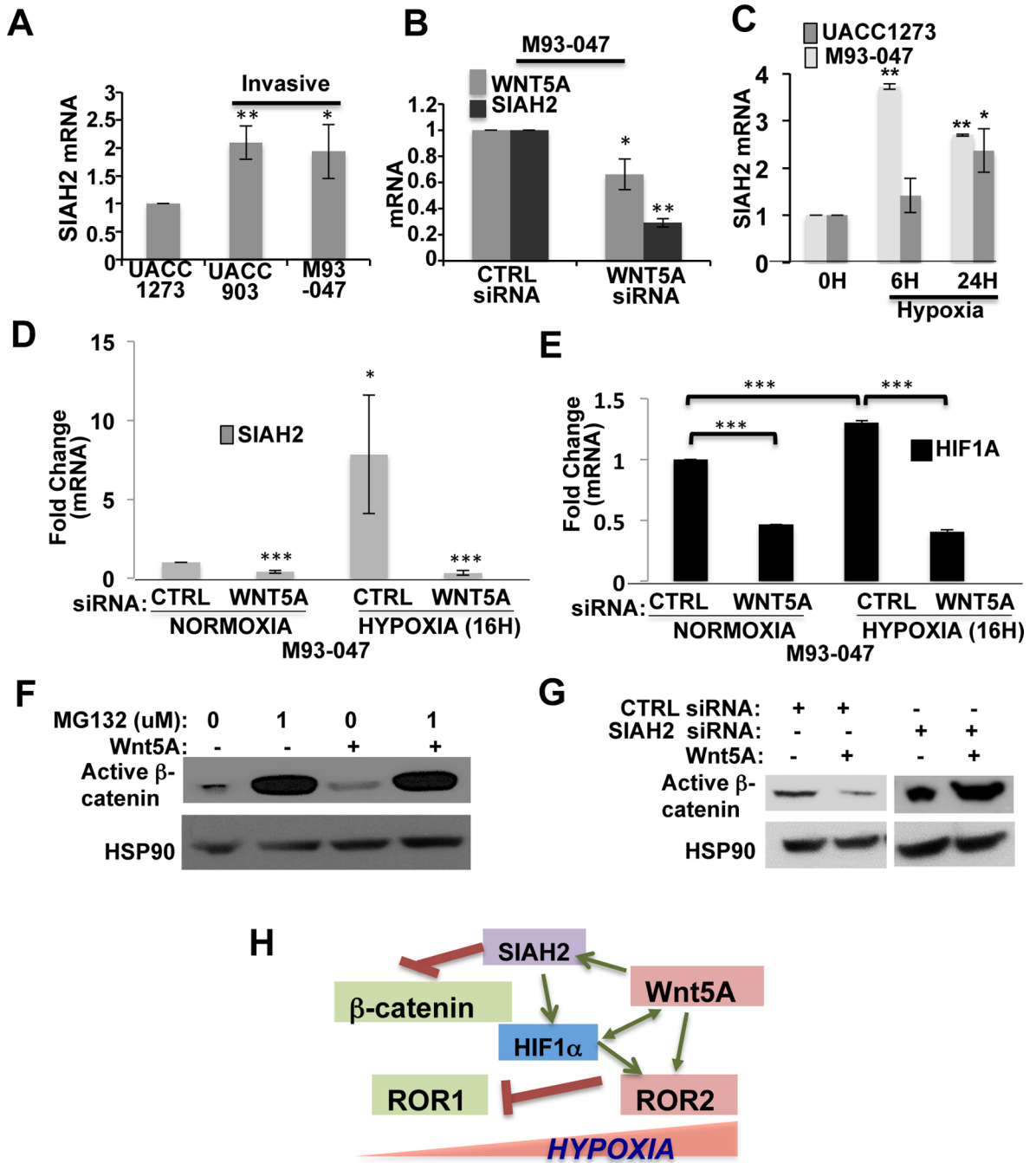


Figure 5. Wnt5A Degrades β-Catenin and Stabilizes HIF1α via Siah2

(A) Analysis of Siah2 mRNA levels in melanoma cells that are increasingly invasive (*p<0.05, **p<0.01; error bars=STDEV). (B) Analysis of Wnt5A and Siah2 mRNA levels by real-time PCR in M93-047 cells treated with either a CTRL or Wnt5A siRNA (*p<0.05, **p<0.01; error bars=STDEV). (C) Siah2 mRNA levels in poorly (UACC1273) and highly (M93-047) invasive melanoma cells following exposure to hypoxia (2% O₂, 6 hours and 24 hours) (*p<0.05, **p<0.01; error bars=STDEV). (D) Siah2 mRNA levels following treatment with CTRL or Wnt5A siRNA in M93-047 cells under normoxic or hypoxic conditions (2% O₂, 24 hours) (*p<0.05, **p<0.01). (E) HIF1α mRNA levels in M93-047 cells following treatment with CTRL or Wnt5A siRNA under normoxic or hypoxic

conditions (2% O₂, 24 hours) (**p<0.01; error bars=STDEV). (F) Expression of active β -catenin in cells following pre-treatment with the proteasome inhibitor (MG132, 10 μ M, 1 hour) in the presence or absence of rWnt5A (200 ng/ml, 16 hours). (G) Expression of active β -catenin in cells after knockdown of SIAH2 (20nM, 48h) in the presence or absence of rWnt5A (200 ng/ml, 16 hours). (H) Schematic representation of hypoxic induction of Wnt5A, Siah2, HIF1 α and ROR2 and subsequent inhibition of β -catenin.

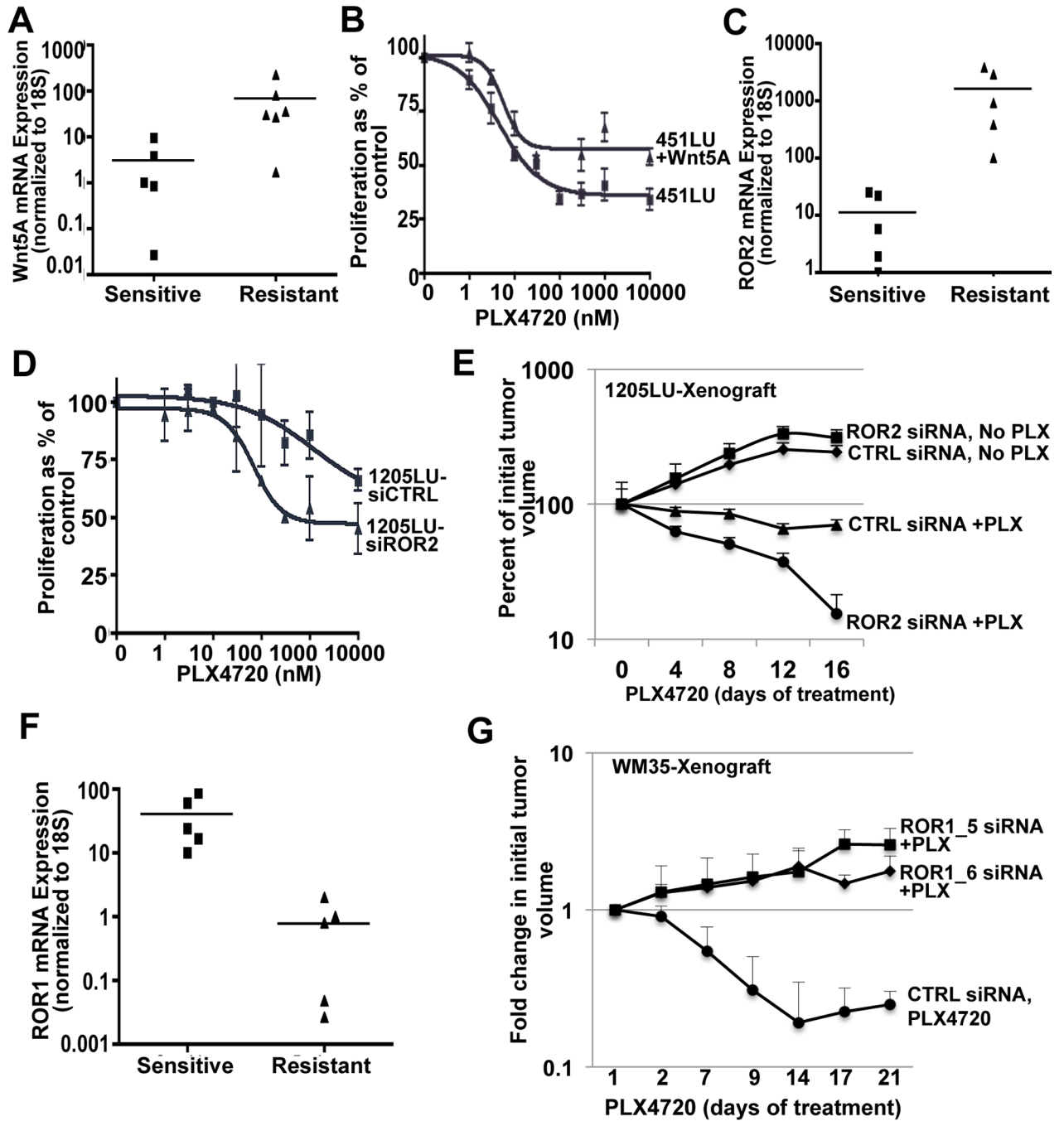


Figure 6. Wnt5A and ROR2 Contribute to Intrinsic Resistance to BRAF Inhibitors

(A) Wnt5A and (C) ROR2 mRNA levels in sensitive and resistant melanoma cell lines analyzed by real-time PCR (* $p < 0.05$, and ** $p < 0.005$, respectively). (B) PLX-sensitive 451LU melanoma cells were treated with increasing doses of PLX4720 and proliferation was analyzed by an MTS assay. (D) PLX-resistant 1205LU cells were transfected with CNTR1 or ROR2 siRNA, and were then treated with increasing doses of PLX4720. (E) Tumor volume analysis in athymic nude mice injected with 1205LU cells transfected with CTRL or ROR2 siRNA. Once tumor formation had occurred (~200 mm³), mice were fed either control AIN-76A chow or AIN-76A chow containing 417 mg/kg PLX4720 and tumors were tracked for 16 days. The percent change in tumor volume was recorded. (F)

ROR1 mRNA levels in sensitive and resistant melanoma cell lines analyzed by real-time PCR (** $p < 0.005$). (G) Tumor volume analysis in athymic nude mice injected with WM35 cells transfected with CTRL or ROR1 siRNA. Once tumor formation had occurred, mice were fed either control AIN-76A chow or AIN-76A chow containing 417 mg/kg PLX4720 and tumors were tracked for 21 days. The change in tumor volume was recorded.

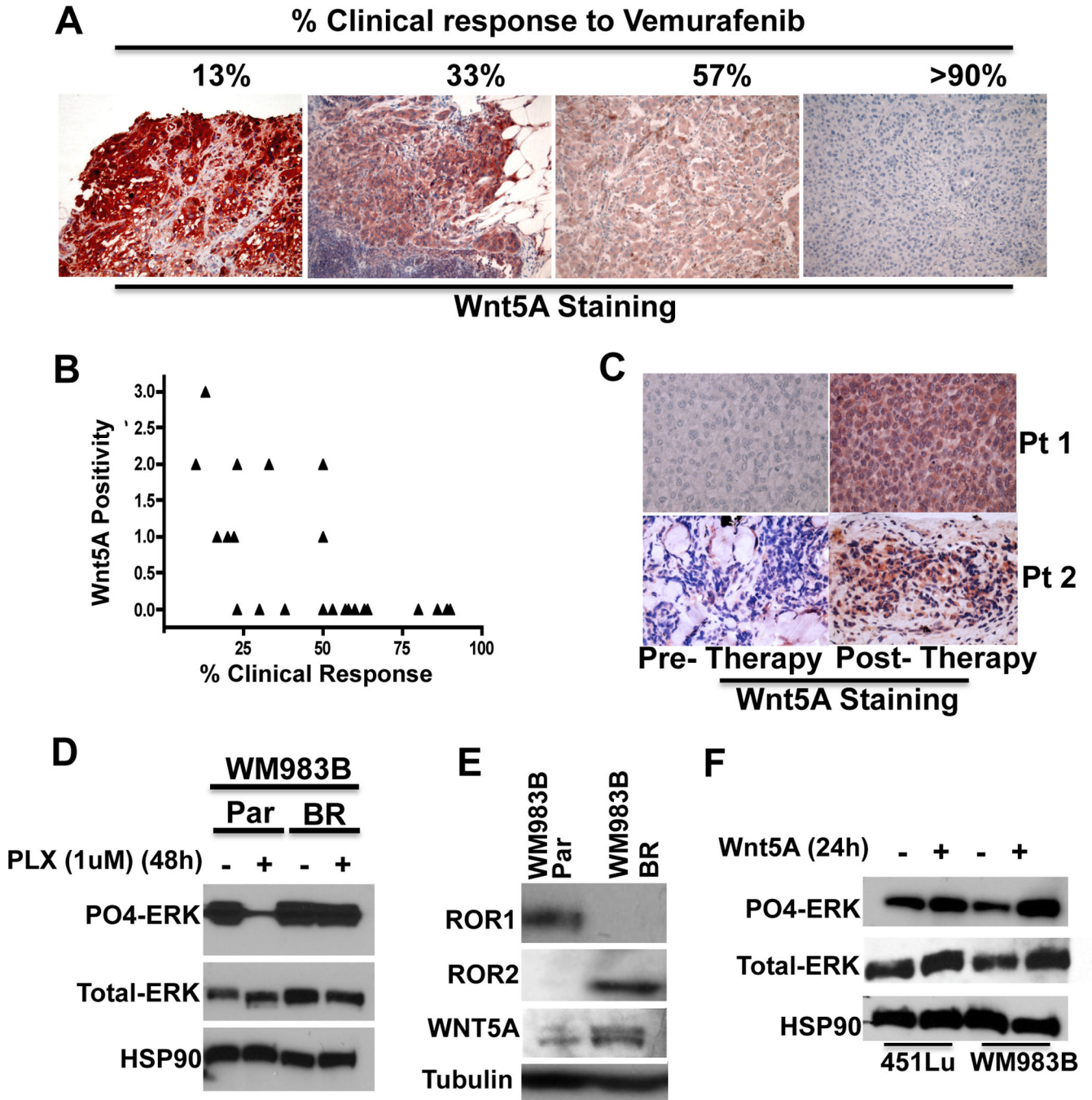


Figure 7. Wnt5A and ROR2 Contribute to Acquired Resistance to BRAF Inhibitors
 (A) Immunohistochemical staining of Wnt5A in 4 different patient samples pre-Vemurafenib treatment. (B) Wnt5A expression was scored and correlated to clinical response following treatment with Vemurafenib. Wnt5A expression correlates to poor patient response (** $p < 0.01$). (C) Immunohistochemical staining of Wnt5A in patient samples pre- and post-treatment with Vemurafenib or Vemurafenib/Trametinib. Wnt5A expression increases in relapsing tumors ($p < 0.05$) (D) Western blot analysis of PO4-ERK and total-ERK expression in WM983B melanoma cells that are sensitive to BRAF inhibitors (parental (Par)) and in resistant (BR) subclones of the parental WM983B cells. Cells were untreated or treated with the BRAF inhibitor PLX4720 (1 μ M, 48 hours). (E) ROR1, ROR2

and Wnt5A protein expression in parental and resistant WM983B cells analyzed by Western blot. (F) Western blot analysis of PO4-ERK and total-ERK expression in WM983B parental cells treated with rWnt5A (200 ng/ml) for 24 hours.